

Ca II K polarization as a diagnostic of temperature bifurcation

R. Holzreuter¹, D. M. Fluri¹, and J. O. Stenflo^{1,2}

¹ Institute of Astronomy, ETH Zurich, 8092 Zurich, Switzerland
e-mail: [holzreuter; fluri; stenflo]@astro.phys.ethz.ch

² Faculty of Mathematics & Science, University of Zurich, 8057 Zurich, Switzerland

Received 10 January 2006 / Accepted 2 February 2006

ABSTRACT

Aims. We compute the linearly polarized spectrum of Ca II K caused by coherent scattering and exploit the line for chromospheric diagnosis, with particular attention to temperature bifurcation, by comparing the theory with solar observations.

Methods. We numerically solve the statistical equilibrium equations and the radiative transfer equation taking into account polarized coherent scattering with partial frequency redistribution. All calculations are performed in 1D within a plane-parallel atmosphere.

Results. We find strong evidence of a chromospheric temperature bifurcation. This suggests that the linearly polarized spectrum of Ca II K might become a valuable tool to study cool components and the dynamics of the chromosphere independently of observations of molecular CO lines and millimeter and sub-millimeter continua.

Key words. line: formation – polarization – radiative transfer – scattering – Sun: chromosphere – Sun: magnetic fields

1. Introduction

The paradigm of a ubiquitous temperature rise in the low chromosphere of the Sun has been substantially impacted by observations of CO molecular lines (Noyes & Hall 1972; Ayres & Testerman 1981; Uitenbroek et al. 1994). The presence of CO lines implies chromospheric regions with temperatures as low as 3700 K, much lower than previously believed. More recent model calculations (Carlsson & Stein 1992, 1994, 1997; Skartlien 2000; Skartlien et al. 2000; Wedemeyer et al. 2003, 2004) give clear hints of a temperature bifurcation in the lower chromosphere with minimum temperatures even below 3000 K. From these calculations, large temporal and spatial fluctuations of the local temperature due to upwards propagating shock waves were derived.

Observational evidence for cool chromospheric components was obtained almost exclusively from CO lines. Some open questions still remain in the modeling of these lines, especially concerning the time dependent dissociation of the CO molecules. Together with contradicting observations, this is reason for ongoing debate about its proper interpretation (Kalkofen 2001; Ayres 2002). Loukitcheva et al. (2004) discuss the need for independent temperature sensitive observables with their attempt to measure and model the millimeter and sub-millimeter continua but they were unable to provide conclusive answers to the open questions.

We investigate the potential of scattering polarization in strong lines as a tool for independent confirmation of cool

components in the solar chromosphere. The linearly polarized spectrum caused by coherent scattering, also known as the “second solar spectrum”, is a very sensitive measure of anisotropy and inhomogeneities in the atmosphere (e.g. Holzreuter et al. 2005). First observations of scattering polarization in strong chromospheric lines date back to Wiehr (1975, 1978) and Stenflo et al. (1980, 1983a,b). The UV version of the Zurich imaging polarimeter ZIMPOL (Gandorfer et al. 2004) can reach a polarimetric accuracy of 10^{-5} in the optical and the near UV. Such a powerful observational tool combined with the recent numerical and theoretical developments (Rees & Saliba 1982; Saliba 1985; Faurobert-Scholl 1992; Landi Degl’Innocenti 1998; Fluri et al. 2003; Holzreuter et al. 2005) allow us to use strong chromospheric lines as a diagnostic indicator.

In this paper we present calculations of scattering polarization in the Ca II K line computed for different model atmospheres. We study the temperature sensitivity of the line and compare computed profiles with observations from Gandorfer (2002).

2. Modeling line polarization

We performed the computations for plane-parallel 1-dimensional model atmospheres with the same modeling strategy as in Holzreuter et al. (2005) where a detailed formulation of the radiative transfer involved may be found.

The polarized spectrum is computed in two major modules. In the first step we compute intensity, opacities and collisional rates neglecting any polarization. We employ the PRD-capable MALI-code developed by Uitenbroek (2001), which is based on the formalism of Rybicki & Hummer (1991, 1992) to solve statistical equilibrium equations and the radiative transfer equation self-consistently. In the second step the linearly polarized spectrum due to coherent scattering is calculated assuming that the quantities obtained in the first step (intensity, opacities, collisional rates) remain unaffected by the small degree of polarization. We fully account for quantum interferences between the two upper fine-structure levels of the Ca II H/K lines, which makes the polarizability W_2 frequency dependent, and for partial frequency redistribution (PRD).

To investigate temperature bifurcation we employ a 2-component model based on two atmospheres, namely the average quiet Sun model FALC (Fontenla et al. 1993) and FALX (Avrett 1995, his model M_{CO}) with a cool chromosphere. It has been shown by Avrett (1995, and references therein) that this kind of atmospheric mixture is able to describe mean profiles of CO, Ca II H/K and UV observations simultaneously, although some discrepancies exist in the filling factors.

3. Results

In this section we compare computed polarized spectra of Ca II K with observations published in the atlas of the second solar spectrum (Gandorfer 2002). These observations near the heliographic south pole were obtained by integrating the signal over at least 30 min, averaged along the slit of $200''$, and thus represent both a spatially and temporally averaged spectrum. We try to fit the observed spectra with individual model atmospheres and with a 2-component model. From the comparison with observed data we obtain clear hints of the existence of colder regions above the classical temperature minimum. We study the influence of blend lines, micro- and macro-turbulence and the Hanle effect on the polarized line profile to ensure that the observed spectra cannot be obtained by more simple means from single models.

3.1. Polarized spectra based on single model atmospheres

Theoretical polarized spectra of Ca II K obtained for the warm FALC (solid) and cold FALX (dotted) model atmospheres are displayed in Fig. 1. Both models are unable to fit observations in the vicinity of the line core.

The wing polarization is however well reproduced by both model atmospheres, although FALC seems to give slightly better fits to observations, especially in the blue wing. The large-scale wing polarization was used to accurately determine the heliocentric angle $\mu = \cos \theta = 0.12$ which lies within the uncertainty of the observations (Gandorfer, private communication) and the Van der Waals parameter $\gamma_{VW} = 1.8 \times 10^{-8}$, a value compatible with that of Ayres (1977).

At frequencies near the line core several problems appear. The hotter model FALC is not able to reproduce the slow rise of polarization at K1 (when approaching K1 from the wing), and

the dip in polarization at K2 is far too strong. Moreover, all calculations with “hot” chromospheric 1D models (FALA, FALF, FALP and other common models) share the same general properties in the core of Ca II K, a problem already encountered by Saliba (1985). In strong contrast, the much cooler FALX model is able to explain the increasing polarization around K1 but does not produce any dip at K2. Again, the polarization profile of the FALX model is typical for any “cool” solar model atmosphere (e.g. models from Carlsson & Stein 1997). Note however that the line core polarization is not sensitive to atmospheric temperature and coincides for both models because the radiation field in the upper chromosphere is completely decoupled from the local kinetic temperature.

The surprising discrepancies of the two models can be understood in terms of the anisotropy of the radiation field, which itself results directly from the source function gradient. This is the case because the degree of scattering polarization scales strongly with the anisotropy of the radiation field (Holzreuter et al. 2005). Positive anisotropy leads to positive polarization (by definition parallel to the closest solar limb), negative anisotropy causes negative polarization, and an isotropic radiation field (in the absence of magnetic fields) results in no polarization because no preferred direction exists.

The lower panels of Fig. 1 display the complex depth and frequency dependence of the anisotropy and the total source function in FALC and FALX. In the wings the anisotropies of the two models almost coincide but slowly decrease due to the decreasing source function gradient when approaching the core. Therefore, wing polarization is similar in both models and slowly drops from the wing maximum toward the wing minimum. Very large differences arise at K1 and K2. In the cold FALX model the source function drops steeply with height because of the cold chromosphere, which induces limb darkening and large positive contributions to the anisotropy. On the other hand, in the warm FALC atmosphere the hot chromosphere prevents the total source function from dropping so that the anisotropy becomes strongly negative and subsequently causes the distinct minima with negative polarization at K2. In the line core the anisotropies of the warm and cold models and thus also the polarization coincide again.

3.2. Temperature bifurcation

It is not possible to fit the observed profile with any individual commonly available 1D solar model (in particular the FALA model for the quiet Sun). On the other hand, a 2-component model consisting of a mixture of warm and cold model atmospheres (FALC/FALX = 0.55/0.45) can easily reproduce the main features of the observations (thick line, middle panel of Fig. 1). As mentioned by Saliba (1985) the optical thickness of the chromosphere directly influences the depth of the K2 dip in polarization. Therefore, it might be possible to fit observations with a single model by modifying the temperature curve in the lower chromosphere. However, such a model with a weak chromosphere would not be able to simultaneously reproduce all the observations explained by Avrett (1995).

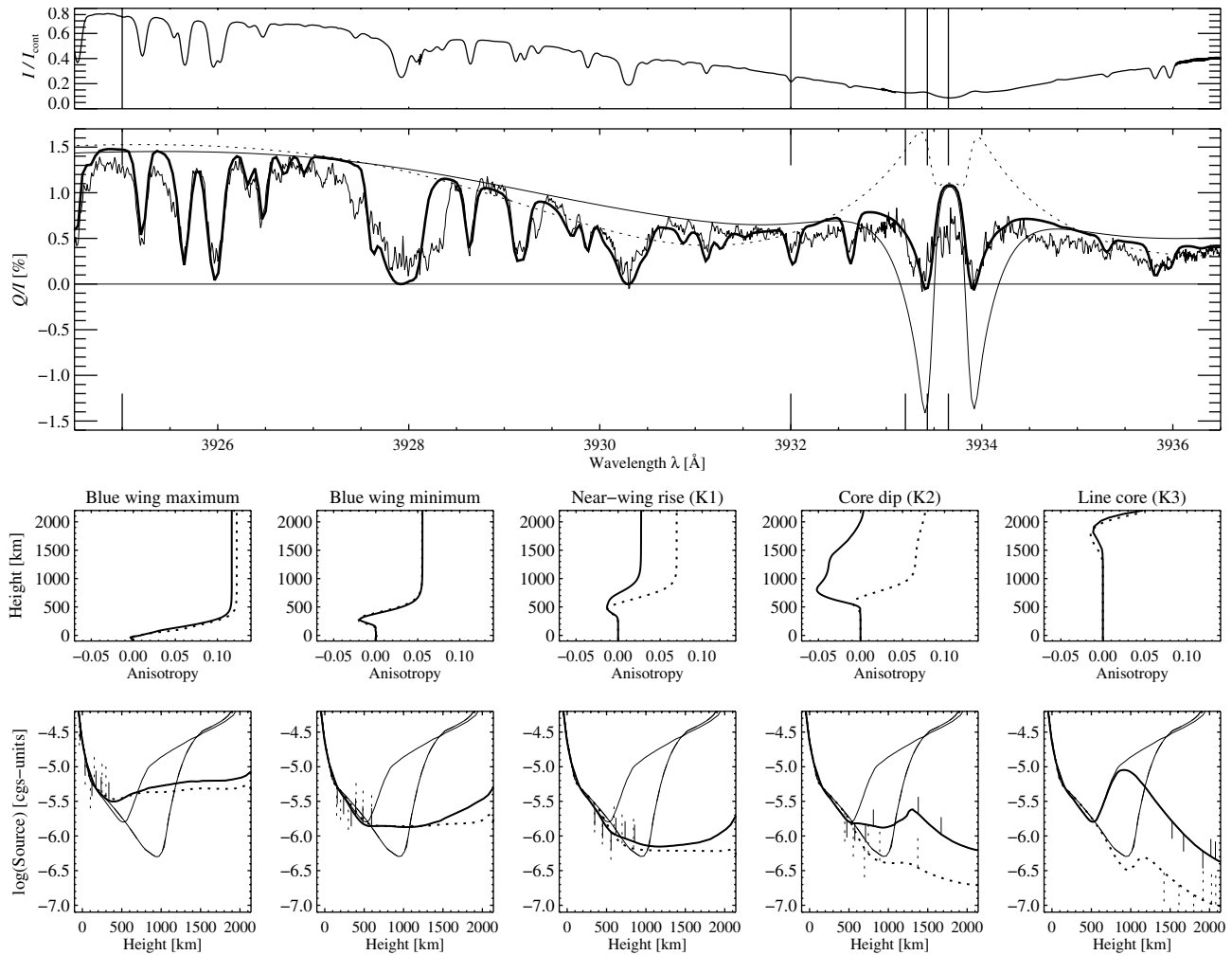


Fig. 1. Evidence of temperature bifurcation in Ca II K. *Top panel:* observed intensity spectrum. *Second panel:* linearly polarized spectrum using the warm FALC model (thin solid, smooth line), the cold FALX model (dotted), the 2-component model with FALC and FALX (filling factor of FALX: 0.45) accounting for depolarizing blends (thick solid), and observations (solid, noisy). *Bottom panels:* depth dependence of the radiation field anisotropy (3rd row) and source functions (4th row) in the FALC (solid) and FALX (dotted) models at indicated wavelengths (3924.98 Å, 3931.99 Å, 3933.20 Å, 3933.43 Å, 3933.66 Å). In the source function plots, the Planck function of the two models is indicated with thin lines. The formation height of the I and Q/I signals is indicated with the three vertical bars which mark the heights where the monochromatic optical depth τ_λ takes the values 3, 1 and 0.3 in the directions $\mu = 0.05$ (upward bars) and $\mu = 0.7$ (downward bars). Note that the difference of the source function between the two directions is a good indicator of the anisotropy at these heights.

In Sects. 3.3 and 3.4 we investigate the different factors that could significantly change the polarization signature near the line core to ensure that single atmospheric models are insufficient to explain the observations.

3.3. Influence of blends, micro- and macro-turbulence

Smearing by macro-turbulence is too small to turn e.g. the FALC result into the observed profile. We have estimated the macro-turbulence parameter (Gaussian, 70 mÅ) from the width of photospheric blends in the wing. Note that the polarization dips at K2 do not result from blend lines, as shown by our calculations, despite having neglected molecular opacity and intrinsic line polarization in the blends.

A larger micro-turbulence leads to a certain weakening of the K2 dips but then their wavelength position is unrealistically shifted towards the wings. In particular, micro-turbulence

does not influence the rise in polarization near K1, which gives further support for the presence of a temperature bifurcation. Micro-turbulence is of course a strong simplification of 1D models and future investigations should include a more realistic simulation.

3.4. Depolarization in the line core via the Hanle effect

Magnetic fields modify scattering polarization in the line core via the Hanle effect, which we have implemented in our code in the same way as in Faurobert-Scholl (1992). We have assumed turbulent magnetic fields (filling factor 100%) with a single field strength value for all heights. This leads to a depolarization of the line core polarization. From Fig. 2 we find that the 2-component model best reproduces observations for magnetic fields of about 8 G.

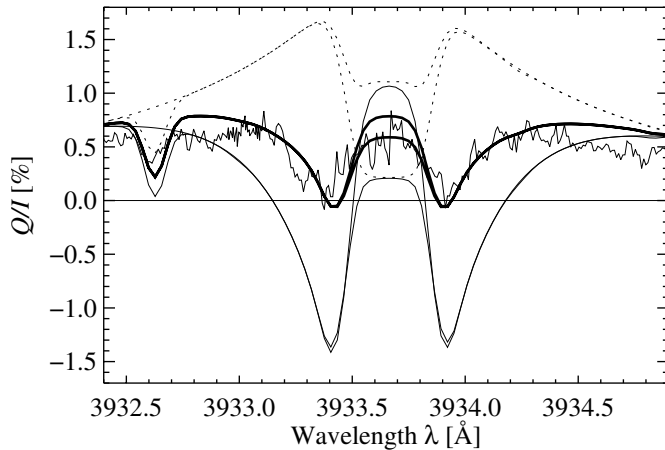


Fig. 2. Depolarization in the core of Ca II K due to the Hanle effect with a turbulent magnetic field. Dotted lines: FALX model for $B = 0$ G and $B = 100$ G (saturated regime). Thin solid, smooth lines: FALC model for $B = 0$ G and $B = 100$ G. Thick solid lines: 2-component model with $B = 6$ G (upper) and $B = 10$ G (lower curve).

However the Hanle effect leaves the polarization dips at K2 nearly unaffected and does not modify the polarization rise at K1. Therefore, it is impossible to obtain the observed profile either from FALC or FALX individually by adding magnetic fields. Only when considering very large atmospheric velocities, can magnetic fields produce variations of the K2 minimum polarization, as reported by Stenflo (2006). This aspect should be addressed in future work.

4. Conclusions

We have established the Ca II K linear scattering polarization as a sensitive diagnostic of atmospheric structure in the upper photosphere and low chromosphere. A comparison using standard 1D models and spatially and temporally averaged observations shows that no single standard 1D model can explain the observed second solar spectrum near the Ca II K core. This confirms the existence of colder regions in the layers above the classical temperature minimum. Higher in the chromosphere, above about 1000 km, scattering polarization in the Ca II K line is not sensitive to the temperature structure. However, the fit of the line core to observations is optimized by the presence of a turbulent magnetic field of 8 G in the upper chromosphere. We can conclude that scattering polarization in Ca II K may indeed be used as a tool to diagnose cold chromospheric regions independently of CO observations. Therefore, better modeling of this line (including 3D calculations) are needed, as is the development of instruments so that spectropolarimetric observations with very high spatial and temporal resolution may be achieved.

Acknowledgements. We thank Han Uitenbroek for providing his RH-code, with which we have computed intensities, and Achim Gandorfer for supplying his atlas of scattering polarization in electronic form. R.H. appreciates the flexibility of Prof. Dr. Norbert Dillier concerning the working hours at the University Hospital of Zurich. We are grateful for the suggestions of the referee that helped us to improve the manuscript.

References

- Avrett, E. H. 1995, in *Infrared tools for Solar Astrophysics: What's Next*, ed. J. R. Kuhn, & M. J. Penn (Singapore: World Scientific), 303
- Ayres, T. R. 1977, *ApJ*, 213, 296
- Ayres, T. R. 2002, *ApJ*, 575, 1104
- Ayres, T. R., & Testerman, L. 1981, *ApJ*, 245, 1124
- Carlsson, M., & Stein, R. F. 1992, *ApJ*, 397, L59
- Carlsson, M., & Stein, R. F. 1994, in *Chromospheric Dynamics*, ed. M. Carlsson, 47
- Carlsson, M., & Stein, R. F. 1997, *ApJ*, 481, 500
- Faurobert-Scholl, M. 1992, *A&A*, 258, 521
- Fluri, D. M., Holzreuter, R., Klement, J., & Stenflo, J. O. 2003, in *Solar polarization*, Proc. 3rd SPW, ed. J. Trujillo Bueno, & J. Sánchez Almeida, ASP Conf. Ser., 307, 263
- Fontenla, J. M., Avrett, E. H., & Loeser, R. 1993, *ApJ*, 406, 319
- Gandorfer, A. 2002, *The Second Solar Spectrum*, Vol. II: 3910 Å to 4630 Å (Zurich: VdF), ISBN No. 3 7281 2844 4
- Gandorfer, A. M., Povel, H. P., Steiner, P., et al. 2004, *A&A*, 422, 703
- Holzreuter, R., Fluri, D. M., & Stenflo, J. O. 2005, *A&A*, 434, 713
- Kalkofen, W. 2001, *ApJ*, 557, 376
- Landi Degl'Innocenti, E. 1998, *Nature*, 392, 256
- Loukitcheva, M., Solanki, S. K., Carlsson, M., Stein, R. F., & Landi Degl'Innocenti, E. 2004, *A&A*, 419, 747
- Noyes, R. W., & Hall, D. N. B. 1972, *BAAS*, 4, 389
- Rees, D. E., & Saliba, G. J. 1982, *A&A*, 115, 1
- Rybicki, G. B., & Hummer, D. G. 1991, *A&A*, 245, 171
- Rybicki, G. B., & Hummer, D. G. 1992, *A&A*, 262, 209
- Saliba, G. J. 1985, *Sol. Phys.*, 98, 1
- Skartlien, R. 2000, *ApJ*, 536, 465
- Skartlien, R., Stein, R. F., & Nordlund, Å. 2000, *ApJ*, 541, 468
- Stenflo, J. O. 2006, in *Solar Polarization*, Proc. 4th SPW, ed. R. Casini, & B. W. Lites, ASP Conf. Ser., in press
- Stenflo, J. O., Baur, T. G., & Elmore, D. F. 1980, *A&A*, 84, 60
- Stenflo, J. O., Twerenbold, D., & Harvey, J. W. 1983a, *A&AS*, 52, 161
- Stenflo, J. O., Twerenbold, D., Harvey, J. W., & Brault, J. W. 1983b, *A&AS*, 54, 505
- Uitenbroek, H. 2001, *ApJ*, 557, 389
- Uitenbroek, H., Noyes, R. W., & Rabin, D. 1994, *ApJ*, 432, L67
- Wedemeyer, S., Freytag, B., Steffen, M., Ludwig, H.-G., & Holweger, H. 2003, *AN*, 324, 410
- Wedemeyer, S., Freytag, B., Steffen, M., Ludwig, H.-G., & Holweger, H. 2004, *A&A*, 414, 1121
- Wiehr, E. 1975, *A&A*, 38, 303
- Wiehr, E. 1978, *A&A*, 67, 257